Altered thalamocortical rhythmicity and connectivity in mice lacking $Ca_V3.1$ T-type Ca^{2+} channels in unconsciousness

Soonwook Choi[a,b], Eunah Yu[a,b], Seongwon Lee[c], and Rodolfo R. Llinás[a,b,1]

[a]Department of Neuroscience and Physiology, New York University School of Medicine, New York, NY 10016; [b]Marine Biological Laboratory, Woods Hole, MA 02543; and [c]Department of Mathematics, Pohang University of Science and Technology, Pohang 790-784, Republic of Korea

Edited by Tomas Hokfelt, Karolinska Institutet, Stockholm, Sweden, and approved May 5, 2015 (received for review November 2, 2014)

In unconscious status (e.g., deep sleep and anesthetic unconsciousness) where cognitive functions are not generated there is still a significant level of brain activity present. Indeed, the electrophysiology of the unconscious brain is characterized by well-defined thalamocortical rhythmicity. Here we address the ionic basis for such thalamocortical rhythms during unconsciousness. In particular, we address the role of $Ca_V3.1$ T-type Ca^{2+} channels, which are richly expressed in thalamic neurons. Toward this aim, we examined the electrophysiological and behavioral phenotypes of mice lacking $Ca_V3.1$ channels ($Ca_V3.1$ knockout) during unconsciousness induced by ketamine or ethanol administration. Our findings indicate that $Ca_V3.1$ KO mice displayed attenuated low-frequency oscillations in thalamocortical loops, especially in the 1- to 4-Hz delta band, compared with control mice ($Ca_V3.1$ WT). Intriguingly, we also found that $Ca_V3.1$ KO mice exhibited augmented high-frequency oscillations during unconsciousness. In a behavioral measure of unconsciousness dynamics, $Ca_V3.1$ KO mice took longer to fall into the unconscious state than controls. In addition, such unconscious events had a shorter duration than those of control mice. The thalamocortical interaction level between mediodorsal thalamus and frontal cortex in $Ca_V3.1$ KO mice was significantly lower, especially for delta band oscillations, compared with that of $Ca_V3.1$ WT mice, during unconsciousness. These results suggest that the $Ca_V3.1$ channel is required for the generation of a given set of thalamocortical rhythms during unconsciousness. Further, that thalamocortical resonant neuronal activity supported by this channel is important for the control of vigilance states.

electroencephalogram | local field potential | mediodorsal thalamus | coherence

Thalamocortical interactive rhythmic activities are well-defined physiological correlates of both conscious and unconscious conditions (1, 2). From a functional perspective, abnormal slow cortical rhythms and their synchronized network dynamics are omnipresent correlates of unconscious states, such as coma and general anesthesia (3, 4). Moreover, a dynamic alteration of coherence as well as coupling/uncoupling in thalamocortical circuits also can be characterized as likely correlates of unconsciousness (3–5).

Since the discovery of low threshold, T-type Ca^{2+} channels (6, 7) and the subsequent studies of intrinsic electrophysiological properties in the thalamic neurons (8, 9), T-type Ca^{2+} channels have been implicated in many physiological and pathological brain states (for a review, see ref. 10). The ionic conductances they support have been shown to generate synchronized oscillatory activity in thalamocortical circuits through calcium-dependent low-threshold spikes (LTSs). Indeed, these LTSs, generated by "deinactivation" of T-type Ca^{2+} channels, underlie thalamic burst firing. This activity is reflected as high-amplitude low-frequency oscillations in electroencephalography, and its presence is recognized as spike-wave-discharges, low-frequency rhythms (<1 Hz slow, delta and theta rhythms), as well as by spindle-generated rhythmicity (10).

Recent molecular genetic studies coupled with electrophysiological and behavioral approaches confirmed the classical view that $Ca_V3.1$ channels play a central role in the generation of thalamocortical rhythms, such as 3- to 4-Hz spike-wave discharge during absence seizures (11, 12). Regarding the role of $Ca_V3.1$ in slow wave sleep, however, mice with such genetic deletions present electrophysiological consequences that are inconsistent with the above generalization, even with behavioral phenotypes exhibiting fragmented sleep. Indeed, mice with a global $Ca_V3.1$ deletion showed reduced delta rhythm (13) in contrast to the increased delta rhythms found in mice with thalamus-restricted deletion of $Ca_V3.1$ (14). In addition, there is clear evidence that thalamic T-type Ca^{2+} channels support the generation of spindle oscillations (15). However, recently published work proposes that sleep spindles are sustained in mice lacking $Ca_V3.1$ channels (16). These results differ from the classical view and raise the need to examine further the role of thalamic $Ca_V3.1$ channels in the generation of thalamocortical rhythms.

Here we addressed the issue of whether $Ca_V3.1$ channels are important for the generation of low-frequency thalamocortical rhythms during unconsciousness. Spectral analysis of EEG recordings from $Ca_V3.1$ KO mice indicates a shift away from low frequency, with an increase probability toward the high-frequency rhythmic components. There is also a significant alteration of thalamocortical dynamic interactions.

Significance

Defining the neuronal activity underlying unconscious states is a fundamental prerequisite to understanding cognitive brain function. The present findings indicate that the neuronal activity associated with unconsciousness is directly related to the voltage-gated ionic conductances supporting thalamic low-frequency electrical oscillations. In particular, voltage-gated calcium channels are important players in the generation of prolonged unconsciousness. Thus, mice with a deletion of voltage-gated $Ca_V3.1$ channels are incapable of maintaining the low-frequency oscillatory activity associated with unconsciousness. These results indicate that $Ca_V3.1$, though functionally very significant in the generation of physiological unconsciousness, is not the only channel involved in the generation of the low-frequency spontaneous brain activity that supports nonpathological unconsciousness.

Author contributions: S.C., E.Y., and R.R.L. designed research; S.C. and E.Y. performed research; S.C., E.Y., S.L., and R.R.L. analyzed data; and S.C. and R.R.L. wrote the paper.

The authors declare no conflict of interest.

This article is a PNAS Direct Submission.

Freely available online through the PNAS open access option.

[1]To whom correspondence should be addressed. Email: rodolfo.llinas@nyumc.org.

This article contains supporting information online at www.pnas.org/lookup/suppl/doi:10.1073/pnas.1420983112/-/DCSupplemental.

Results

The initial steps in this study addressed EEG recordings and their spectral profiles. The classical finding, that during unconsciousness spectral profiles differ significantly from those recorded in the conscious status, is confirmed. Thus, during unconsciousness, high-amplitude low-frequency oscillations (delta, 1–4 Hz) were markedly increased from the awake state when unconsciousness was induced by ketamine (Fig. S1 *A–D*) or by ethanol (Fig. S1 *E–H*). The delta power was significantly increased in the spectral analysis of absolute power (Fig. S1 *B*, *C*, *F*, and *G*). The percentage of delta band, which was calculated in reference to the power of the entire EEG spectrum, also significantly increased (Fig. S1 *D* and *H*). The robustly increased delta and the largely decreased theta, alpha, beta, and gamma in the spectral distribution of relative power are independent of the agent used to trigger unconsciousness (cf. Fig. S1 *D* and *H*).

Reduced Low-Frequency and Increased High-Frequency Oscillations in $Ca_V3.1$ KO Mice During Unconsciousness. To assess the role of $Ca_V3.1$ channels in the alteration of EEGs during unconsciousness, we examined the overall spectral profile of EEGs after high-dose injection of ketamine (120 mg/kg) or ethanol (3.5 g/kg), both of which are known to induce unconscious status. EEGs were recorded from frontal (FCx) and parietal cortex (PCx) of WT mice and KO mice using epidural electrodes. The effects of ketamine or ethanol on the EEG were studied 5–15 min after injection of ketamine or ethanol, a time window for anesthetic unconsciousness. The mean spectral power was calculated from 5-min epochs for each animal. Administration of ketamine, an NMDA receptor antagonist, increased low-frequency oscillatory activity over pre-administration levels in both KO and WT mice (Fig. 1 *A–C*; see Fig. S1 *A–D* for control). However, the increase in mean absolute power (Fig. S2*A*) and the accumulated absolute power of delta band (Fig. 1*B*) were less marked in KO than in WT mice, and this was particularly true in FCx, when KO and WT mice were compared [one-way ANOVA $F(1, 15) = 7.557$ and $P < 0.05$]. The proportion of delta band was also significantly lower in KO than WT mice (Fig. 1*C*) in both FCx [one-way ANOVA $F(1, 15) = 11.709$ and $P < 0.01$] and PCx [one-way ANOVA $F(1, 15) = 5.543$ and $P < 0.05$]. In addition to the reduction in delta band oscillations, both in absolute and relative value of spectral power, a fundamental difference was encountered in the EEG spectral power between KO and WT. The absolute spectral power of high-frequency oscillations, such as beta and gamma band, was higher in KO mice [Fig. 1*B*; β in FCx, one-way ANOVA, $F(1, 15) = 5.178$, $P < 0.05$; β in PCx, one-way ANOVA, $F(1, 15) = 6.875$, $P < 0.05$; γ in FCx, one-way ANOVA, $F(1, 15) = 6.463$, $P < 0.05$; γ in PCx, one-way ANOVA $F(1, 15) = 7.119$ and $P < 0.05$]. The percentage of beta band was also higher in KO than in WT in both frontal and parietal cortex [Fig. 1*C*; FCx, Kruskal–Wallis test, $P < 0.01$; PCx, one-way ANOVA, $F(1, 15) = 9.022$, $P < 0.01$]. Relative power of gamma band was higher in KO than WT mice only in FCx (Fig. 1*C*; Kruskal–Wallis test, $P < 0.01$).

These results were compared with unconsciousness induced by ethanol in KO and WT mice. Ethanol is classified as a $GABA_A$ receptor-positive allosteric modulator. The alterations in EEG profiles during ethanol-induced unconsciousness were similar to those during ketamine-induced unconsciousness. However, the changes in amplitude and frequency were significantly smaller compared with those following ketamine administration (Fig. 1 *A* and *D*; also note scale difference in Fig. 1 and Fig. S2). Compared with WT, the lowered delta oscillation of KO mice was observed only in the frontal cortex during ethanol-induced unconsciousness (Fig. 1 *D–F* and Fig. S2*B*). The delta band in FCx of KO was lowered both in absolute power (Fig. 1*E*; Kruskal–Wallis test, $P < 0.05$) and in relative power [Fig. 1*F*; one-way ANOVA, $F(1, 15) = 13.515$, $P < 0.01$]. The mean absolute spectral power of gamma band was higher in KO mice [Fig. 1*E*; γ in FCx, one-way ANOVA, $F(1, 15) = 9.579$, $P < 0.01$; γ in PCx, one-way ANOVA, $F(1, 15) = 6.561$, $P < 0.05$]. Also, the contribution of activity in the high-frequency bands to total activity was significantly higher in KO than in WT mice (Fig. 1*F*). This

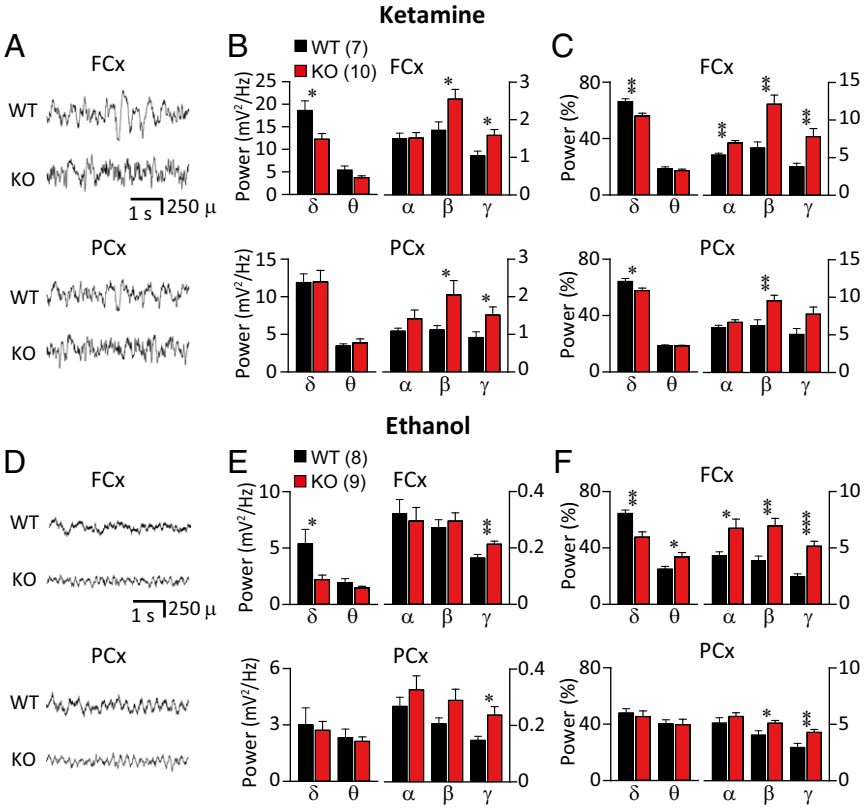

Fig. 1. Effect of unconsciousness induced by ketamine (*A–C*, 120 mg/kg, i.p.) or ethanol (*D–F*, 3.5 g/kg, i.p.) on EEG spectrum in $Ca_V3.1$ KO and WT mice. Reduced low-frequency (delta) and increased high-frequency oscillations (beta and/or gamma) were observed both in absolute and relative value of spectral power of KO, compared with WT. (*A* and *D*) Representative EEG recordings from FCx and PCx. (*B* and *E*) Mean absolute power of accumulated several frequency bands in EEG recordings from FCx and PCx. (*C* and *F*) Relative power of spectral distribution. Frequency bands are represented as follows: delta (δ), 1–4 Hz; theta (θ), 4–8 Hz; alpha (α), 8–12 Hz; beta (β), 12–25 Hz; and gamma (γ), 25–50 Hz. Statistically significant differences marked as $*P < 0.05$, $**P < 0.01$, and $***P < 0.001$, one-way ANOVA.

Table 1. Loss of righting reflex

Anesthetic used (no. of mice)	LORR latency	LORR duration
Ketamine		
WT (12)	160.8 ± 6.3	889.2 ± 86.1
KO (12)	232.5 ± 12.9***	581.7 ± 98.3**
Ethanol		
WT (9)	76.0 ± 5.4	2670.0 ± 165.9
KO (11)	92.7 ± 3.8*	1481.8 ± 165.4**

Latency and duration of LORR as a behavioral measure of unconsciousness. *$P < 0.05$, **$P < 0.01$, ***$P < 0.001$; one-way ANOVA.

difference was most marked in the beta and gamma bands in both FCx and PCx [Fig. 1*F*; β in FCx, one-way ANOVA, $F(1, 15) = 12.329$, $P < 0.01$; β in PCx, one-way ANOVA, $F(1, 15) = 4.747$, $P < 0.05$; γ in FCx, Kruskal–Wallis test, $P < 0.001$; γ in PCx, one-way ANOVA $F(1, 15) = 8.286$ and $P < 0.05$].

Determining whether the frequency profiles shown in Fig. 1 were related to particular aspects of unconsciousness was addressed. Following ketamine administration, the time to induce loss of the righting reflex (LORR; no recovery from supine posture during unconsciousness) was longer in KO than in WT mice (Table 1) [one-way ANOVA, $F(1, 22) = 25.002$, $P < 0.001$]. The total duration of LORR was shorter in KOs than in WT mice (Kruskal–Wallis test, $P < 0.01$). These results demonstrate that ketamine-induced unconsciousness was differentially affected, if not prevented, by the deletion of $Ca_V3.1$ channels. Similarly, the latency to LORR was longer and the total duration of LORR was shorter in KO than in WT mice after ethanol injection (Table 1). Taken together, these results indicate that electrophysiological and behavioral characteristics of pharmacologically evoked unconsciousness were modified by the deletion of $Ca_V3.1$ channels.

$Ca_V3.1$-Mediated Rhythms Indicate Different Thalamocortical Involvement in Frontal and in Parietal Cortices During Unconsciousness. $Ca_V3.1$ channels are mainly expressed in thalamus throughout the nuclei of the dorsal thalamic region (17), which is significant because their activation plays an important role in the generation of rhythms in the cortex through reciprocal thalamocortical recurrent activation. Thus, a comparison of the differential contribution of the frontal and parietal cortices to cortical oscillation during unconsciousness in WT mice can provide a clue to the role of the thalamus in consciousness.

During ketamine-induced unconsciousness, the increase of total power (normalized to baseline) was greater in FCx than in PCx [total in Fig. 2*A*; one-way ANOVA $F(1, 12) = 6.922$ and $P < 0.05$]. This difference was also seen in the mean increase in the accumulated absolute power in the delta frequency range [Fig. 2*A*; one-way ANOVA $F(1, 12) = 6.367$ and $P < 0.05$]. The mean decrease in relative beta band power [one-way ANOVA $F(1, 12) = 7.035$ and $P < 0.05$] and gamma band power [one-way ANOVA $F(1, 12) = 8.753$ and $P < 0.05$] was significantly larger in FCx than in PCx (Fig. 2*B*). Similar results were observed during unconsciousness induced by ethanol. There was a larger increase in total power, and in delta band power in FCx than in PCx (Fig. 2*A*; Kruskal–Wallis test, $P < 0.05$). The decrease in the relative beta and gamma band power was more marked in FCx than in PCx [Fig. 2*B*; β, one-way ANOVA $F(1, 14) = 6.063$ and $P < 0.05$; γ, one-way ANOVA $F(1, 14) = 9.609$ and $P < 0.01$].

The Role of $Ca_V3.1$ in Mediodorsal Thalamic Control of Rhythmicity During Unconsciousness. Given the strong interconnectivity between the mediodorsal (MD) thalamic nuclei and the frontal cortex in mice (18), we examined the characteristics of local field potentials (LFPs) in MD to determine whether rhythmicity characteristics in FCx were related to alteration of rhythmicity in MD during unconsciousness. LFPs were obtained from MD in WT and KO mice after administration of a high dose of either ketamine (Fig. 3 *A* and *B*, and Fig. S3 *A* and *B*) or ethanol (Fig. 3 *C* and *D* and Fig. S3 *C* and *D*). Robust increases in low-frequency oscillations were clearly observed in LFPs from the MD in WT mice (Fig. 3 and Fig. S3). Although high-amplitude low-frequency oscillations were observed in the MD of KO mice, this was significantly less common than in WT mice. The absolute power of delta band was lower in KO mice than in WT during ketamine-induced unconsciousness [Fig. 3*A*; one-way ANOVA, $F(1, 15) = 10.007$, $P < 0.01$] and during ethanol-induced unconsciousness (Fig. 3*C*; Kruskal–Wallis test, $P < 0.05$). Analysis of the spectral distribution of MD LFPs also revealed a lower contribution of delta band to total activity in KO mice than that in WT mice during unconsciousness induced by ketamine [Fig. 3*B*; one-way ANOVA, $F(1, 18) = 13.460$, $P < 0.01$] or by ethanol [Fig. 3*D*; one-way ANOVA, $F(1, 14) = 5.298$, $P < 0.05$].

Concerning high-frequency band activity, the contribution of beta and gamma band components was higher in KO than WT mice during unconsciousness induced by ketamine [Fig. 3*B*; β, one-way ANOVA, $F(1, 18) = 13.244$, $P < 0.01$; γ, one-way ANOVA, $F(1, 18) = 7.850$, $P < 0.05$]. During unconsciousness induced by ethanol, alpha and beta band were higher in the MD of KO than in WT mice [Fig. 3*D*; α, Kruskal–Wallis test, $P < 0.01$; β, one-way ANOVA, $F(1, 13) = 7.962$, $P < 0.05$]. Because the alteration of rhythmicity in MD was very similar to that seen in FCx, functional interconnectivity between these regions during unconsciousness is proposed.

Thalamocortical Connectivity Between FCx and MD, via $Ca_V3.1$, During Unconsciousness. To address the role of $Ca_V3.1$ channels in thalamocortical dynamics, as related to the control of consciousness, we assessed the functional connectivity between FCx and MD. This connectivity was implemented by spectral coherence to quantifying the extent of coupling between the same frequencies (Fig. 4), and bispectral coherence to quantify the extent of coupling between different frequencies (Fig. 5). Unconsciousness in both WT and KO mice was accompanied by a significant alternation in coherence (Fig. 4 *B* and *D*) and in the spectral profile of several frequency bands (Fig. 4 *A* and *C*). Thus, the FCx-MD spectral power coherence in KO mice was compared with WT mice before and after ketamine (Fig. 4*B*) or ethanol (Fig. 4*D*). Two-way ANOVA revealed significant differences between WT and KO mice in FCx-MD spectral coherence during unconsciousness. Notably, the FCx-MD delta band coherence increased in WT after injection of ketamine (Fig. 4*B*, black asterisk; two-way ANOVA multiple comparison Tukey's post hoc analysis, $P < 0.01$) or ethanol (Fig. 4*D*, black asterisk; two-way ANOVA multiple comparison Tukey's post hoc analysis, $P < 0.05$). By contrast, FCx-MD delta band coherence decreased in KO mice after induction by ketamine (Fig. 4*B*, red asterisk; two-way ANOVA multiple comparison Tukey's post hoc analysis, $P < 0.05$) or showed no changed in KO mice after induction by ethanol (Fig. 4*D*). FCx-MD delta band coherence was lower in KO than that of WT during unconsciousness induced by ketamine [Fig. 4*B*, blue asterisk; $F(1, 26) = 17.085$, $P < 0.001$) or ethanol

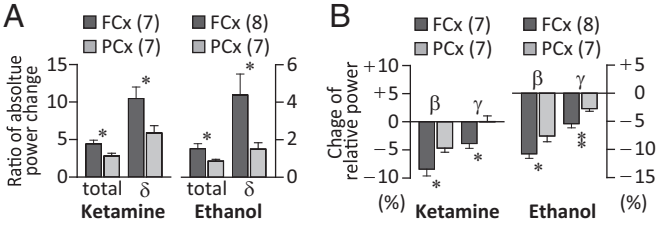

Fig. 2. Differential effect on FCx and PCx rhythmic activity during ketamine- or ethanol-induced unconsciousness. (*A*) Increase in total power and delta power was smaller in PCx than in FCx during unconsciousness induced by ketamine or ethanol. (*B*) Decrease in beta and gamma band was smaller in PCx than in FCx. Statistically significant differences marked as *$P < 0.05$ and **$P < 0.01$ by one-way ANOVA.

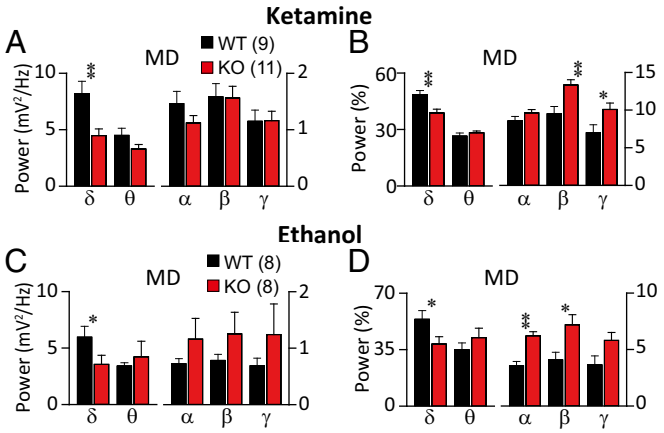

Fig. 3. LFPs and spectral profiles of MD thalamus in $Ca_V3.1$ KO, compared with WT, during unconsciousness induced by ketamine (*A* and *B*) or ethanol (*C* and *D*). (*A* and *C*) Mean absolute power of accumulated several frequency bands in LFP recordings from MD. (*B* and *D*) Relative power of spectral distribution. Absolute and relative spectral distribution showed that during unconsciousness, less low frequency (δ) was observed in MD of KO than WT mice. Statistically significant differences marked as $*P < 0.05$ and $**P < 0.01$ by one-way ANOVA.

(Fig. 4*D*, blue asterisk; $F(1, 26) = 13.468$, $P < 0.001$]. After ketamine, theta and alpha coherence decreased in WT and KO mice, whereas no significant changes were seen in the beta or gamma range (Fig. 4*B*). Decreased theta and alpha coherence reached significance only for the KO mice after ethanol, whereas there was increased coherence for both groups in the gamma range (Fig. 4*D*).

Further analysis was implemented in WT and KO mice by calculating the cross bispectral coherence between FCx and MD, which measures the extent of phase coupling between different frequencies. During unconsciousness induced by ketamine, WT mice exhibited strong bicoherence peaks at frequencies below 10 Hz, both from MD to FCx (Fig. 5*A*, WT) and from FCx to MD (Fig. 5*B*, WT). Though the main peak, in the same low-frequency range, was observed in KO mice, the value of peak coherence was significantly lower than in WT mice (Fig. 5 *A* and *B*, KO, note scales). Other bicoherence peaks were observed only in KO mice. These concerned heterogeneous pairs of broad frequency band biphasic frequencies, especially in the cross-bispectral coherence from MD to FCx (Fig. 5*A*, KO).

Similar characteristics for FCx-MD cross-bispectral coherence were observed during unconsciousness induced by ethanol as follows: (*i*) The main peak appeared in the low-frequency band in both WT and KO mice (Fig. 5 *C* and *D*). (*ii*) A lower value of peak bicoherence was seen in KO than WT mice (Fig. 5 *C* and *D*, note scales). (*iii*) Other bicoherence peaks, in the heterogeneous pairs of other frequency bands, were observed in KO mice (Fig. 5*D*), further supporting the role of $Ca_V3.1$ channels in thalamocortical resonant connectivity.

Discussion

Our results demonstrate the essential role of $Ca_V3.1$ channels in the genesis of low-frequency thalamocortical rhythms, in particular in the 1- to 4-Hz delta frequency band, confirming the classical view regarding the role of T-type Ca^{2+} channels in the thalamocortical loop. We also identified the $Ca_V3.1$ channel as an important player in the molecular basis for consciousness. Indeed, the results reported here indicate that thalamocortical rhythms and their functional coupling, mediated by $Ca_V3.1$ channels, are largely, but not exclusively, responsible for unconscious brain function. Moreover, quite unexpectedly, during unconsciousness, high-frequency oscillations (known as characteristic EEG spectral bands in the aroused state) were increased in mice lacking $Ca_V3.1$ channels, compared with control mice. Taken together, $Ca_V3.1$ T-type Ca^{2+} channel is important for the low-frequency (e.g., delta) and high-frequency (e.g., beta and gamma) rhythms that are related to conscious/unconscious status.

Thalamic burst firing, which is generated by a major contribution from $Ca_V3.1$-mediated LTS, is known to be involved in the generation of low-frequency oscillations (8, 19). It is well known that hyperpolarization, generated by NMDA receptor block, is sufficient to deinactivate T-type Ca^{2+} channels, resulting in rhythmic thalamic bursting (20). By contrast, ethanol, known to elicit thalamic extrasynaptic $GABA_A$-mediated tonic inhibition, also results in their burst firing via membrane hyperpolarization (21). From the above, it follows that in $Ca_V3.1$ KO mice, the reduced delta band activation during unconsciousness, elicited either through a blockage of NMDA receptors (by ketamine administration) or augmentation of $GABA_A$ receptor inhibition (by ethanol administration), can be ascribed to the absence of $Ca_V3.1$ channels and the resulting dynamic consequences—namely, lack of LTS that is consistent with the established role of $Ca_V3.1$ channels in low-frequency thalamocortical oscillations.

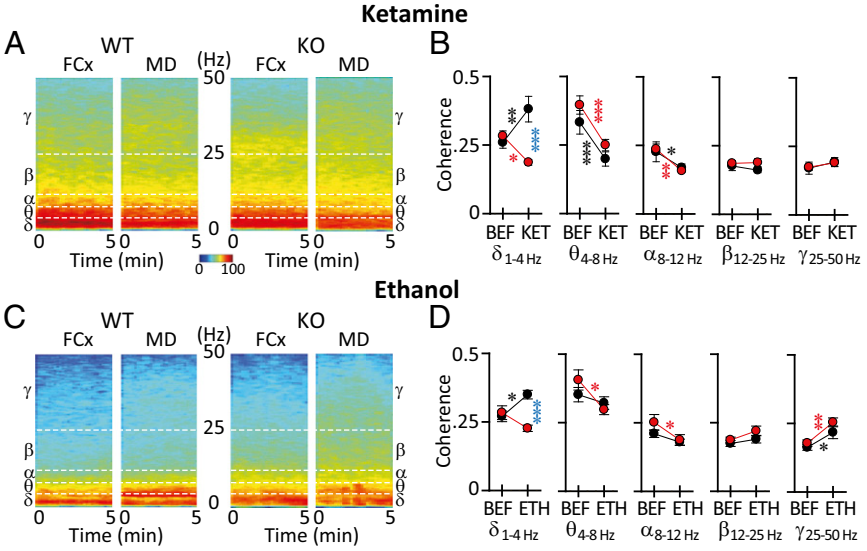

Fig. 4. Spectral coherence of frontal cortex/medial dorsal thalamus (FCx-MD) functional connectivity in WT and KO mice under (*A* and *B*) ketamine- or (*C* and *D*) ethanol-induced unconsciousness. (*A*) Representative power spectrogram for 5 min from FCx and MD in WT and KO mice was calculated under ketamine unconsciousness. (*B*) Plots of coherence before (BEF) and after ketamine (KET) in five frequency ranges. Note that delta coherence increased in WT but decreased in KO mice. (*C*) Same as in *A* under ethanol-induced unconsciousness. (*D*) Plots of coherence before and after (ETH) ethanol-induced unconsciousness. Note differential effect on ethanol on WT and KO mice in the delta range. Number of mice: ketamine, seven WT and eight KO; ethanol, eight WT and seven KO). Statistically significant differences marked as $*P < 0.05$, $**P < 0.01$, and $***P < 0.001$ by two-way repeated-measures ANOVA. Black, before/after change in WT; red, before/after change in KO; blue difference between WT and KO after.

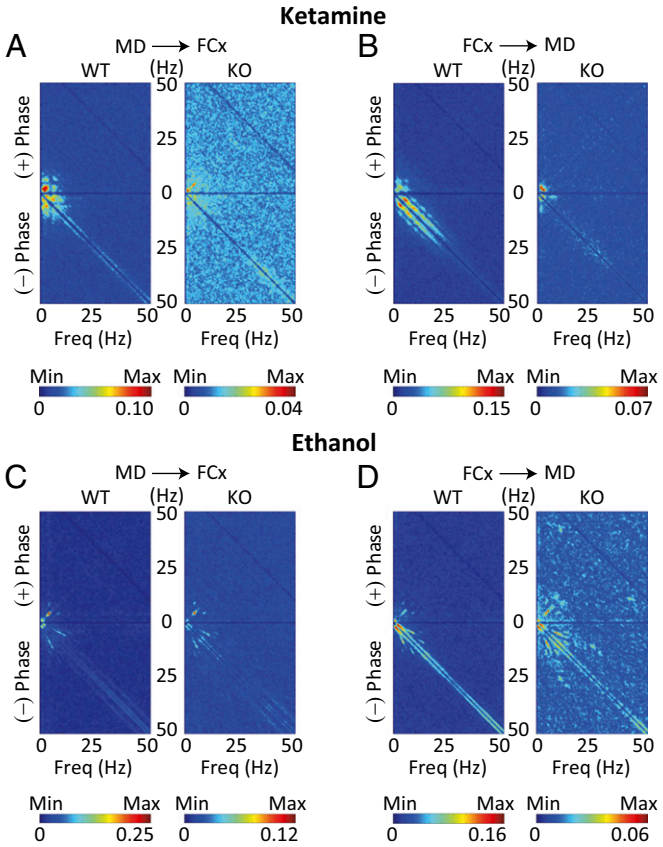

Fig. 5. FCx-MD functional connectivity by cross-bispectral coherence. (*A* and *B*) Averaged cross-bispectral coherence between MD and FCx during unconsciousness induced by ketamine. The value of bicoherence peak was lower in KO than WT mice. Note that the heterogeneous pairs of biphasic frequencies of broad frequency bands were observed only in KO mice, particularly in the cross-bispectral coherence from MD to FCx (see the scattered pattern of peak bicoherence). (*C* and *D*) Same as in *A* and *B* under ethanol-induced unconsciousness. The significantly lowered cross-bispectral coherence in low-frequency band and the heterogeneous pairs of bicoherence in other frequency bands were also observed in KO mice.

Delta rhythm can arise either at thalamic or cortical level. Thalamic delta rhythm generation and the specific neuronal mechanism (ionic conductance by T-type calcium channel) are described in this paper. By contrast, other forms of delta rhythm have characteristics suggesting a purely cortical origin (22); as such, although T-type dependent thalamic delta rhythm arising from the thalamus is not present in $Ca_V3.1$ KO mice, these mice have a certain level of cortically generated delta rhythm indicating thalamocortical resonance, not just thalamic drive. Thus, in unconscious KO mice, local cortical circuits can generate delta rhythms. Because the control of consciousness is not a simple phenomenon, and is crucial for survival, deletion of a single molecular moiety might not be sufficient to eradicate the entire consciousness/unconsciousness rhythmicity. The main conclusion arising from this study is that thalamic $Ca_V3.1$ T-type calcium channels are, most definitively, one of the key molecular mechanisms, but not the only trigger of this fundamental process.

From a cortical perspective, it has been shown that the membrane potential of sparsely spiny inhibitory neurons in cortical layer IV support high-frequency oscillations at gamma band frequencies via low-threshold sodium current activation followed by a potassium conductance (23). The pace-making input of these interneurons onto thalamic projecting pyramidal neurons can result in high-frequency activation of the thalamocortical loop. Considering the increased high-frequency activity in $Ca_V3.1$ KO mice, it is likely that the absence of $Ca_V3.1$ channels may also contribute to high-frequency activation, particularly because $Ca_V3.1$ channels are also expressed in cortex (17). The following should be considered concerning the synchronous firing of inhibitory fast-spiking neurons that impose gamma rhythm on other cells in the network (24, 25). Lack of $Ca_V3.1$ channels in $Ca_V3.1$ KO will affect the firing of fast-spiking inhibitory cells at gamma frequency. The altered interaction between excitatory and inhibitory cortical neurons, induced by ketamine or by ethanol, is probably responsible for the increased beta/gamma cortical oscillation. Indeed, during delta wave sleep, neurons are globally inhibited by GABA (26). By contrast, in unconscious $Ca_V3.1$ KO mice, reduced inhibition of fast-spiking inhibitory interneurons interconnected via GABAergic junctions is expected, and this can be sufficient to generate spike synchronization, with the resulting rhythmic inhibition producing neural ensemble high-frequency oscillations.

Another plausible explanation for the increased high-frequency band activity in $Ca_V3.1$ KO mice is the alteration of the intrinsic electrophysiological properties of thalamic neurons. Indeed, high-frequency oscillations in thalamic neurons have been associated with the generation of high-frequency oscillatory properties in thalamocortical network supported by the activation of dendritic P/Q-type Ca^{2+} channels (27). Previous studies have shown that abnormally large T-type Ca^{2+} currents were encountered with genetic deletion or alteration of the P/Q-type calcium channel (12, 28). Thus, the converse situation, where increased P/Q-type Ca^{2+} channel mediated activities in the absence of T-type Ca^{2+} channels, could also be supported through the compensatory alterations in $Ca_V3.1$ KO mice. This possibility is particularly relevant given that compensatory mechanisms at the cellular level can occur. Thus, it is important to determine whether the $Ca_V3.1$ KO mice phenotypes simply reflect the first-order functionality or the complex outcome of compensatory mechanisms.

Further analysis of adaptive changes at the cellular, synaptic, and circuit levels in $Ca_V3.1$ KO mice will also provide information on the mechanism by which high-frequency thalamocortical oscillations may be increased in these mice. In addition, such studies can shed light on the mechanism responsible for increased delta oscillations (14) and the persistence of spindles (16) in the absence of thalamic $Ca_V3.1$ channels. Although further studies are required regarding the unexpectedly augmented high-frequency oscillations, the $Ca_V3.1$ KO mice represent a useful phenotype in which to investigate the role of high-frequency oscillations in the generation of different consciousness states. Indeed, thalamocortical high-frequency oscillations are omnipresent both in consciousness and unconsciousness states. The central issue here is the attention mechanism that allows particular sensory inputs to be attended to, to be remembered, or even fabricated, as happens in dreams (1). Indeed, in dreaming (mostly REM sleep), high-frequency oscillations are present but are not dependent on sensory input. Thus, the study of phase-reset dynamics both at neuronal and systemic levels in the thalamocortical loops of $Ca_V3.1$ KO mice will be essential in investigating the functional role of high-frequency oscillations in diverse brain states.

In short, the present results indicate that $Ca_V3.1$ channels play an essential role not only in the generation of thalamocortical rhythms but also in its coherent coupling with sensory information known as the basis for sensory evoked conscious experience (1). These findings also address the role of the $Ca_V3.1$ channels in mediating thalamocortical coherence during delta sleep. Concerning the spectral coherence between FCx and MD during anesthetic unconsciousness, it is interesting to note that KO mice exhibited the disrupted thalamocortical coherence of delta band but that the thalamocortical coherence of high-frequency bands were not significantly different from that of WT littermates (Figs. 4 and 5). The basic issue here concerns rhythmic coherence between thalamus and cortex. The functional significance of thalamocortical network coherence relates to the dynamic requirements CNS networks must have to support restful sleep. Clearly, given the importance of such global brain function,

assigning total network oscillations to single-channel activity would be a grave mistake. Indeed, much information is now available about the further sculpting of low-frequency coherence by inhibitory interneuronal networks (24, 29–31).

Also interesting is the fact that $Ca_V3.1$ KO mice show attenuated LORR following ketamine (120 mg/kg, i.p.) or ethanol (3.5 g/kg) administration (Table 1). Though findings appeared to be in conflict with previous results showing no significant changes of LORR following the use of several general anesthetics (32), this discrepancy is most probably due to the difference of exposure or anesthetics dosages used to induce LORR. Although the 50% effective concentration for LORR in $Ca_V3.1$ KO mice was not altered, the latencies to develop LORR of $Ca_V3.1$ KO mice after exposure to anesthetics, such as isoflurane, halothane, sevoflurane, and pentobarbital, were longer (32), which our results have confirmed.

The main focus of our study has been to determine the functional significance of $Ca_V3.1$ channels in generating the thalamocortical delta rhythm, and its interaction with beta/gamma rhythms during unconsciousness, as one of the key molecules to control vigilance states. Ultimately, these results are all in good accordance with the view of the importance of $Ca_V3.1$ T-type Ca^{2+} channel in the generation and maintenance of unconsciousness.

Materials and Methods

Animals. $Ca_V3.1$ null KO mice and their littermate controls (WT) were generated by mating heterozygotes of $Ca_V3.1$ (C57BL/6) from RIKEN BioResource Center (32). Mice were housed with free access to food and water under controlled temperature conditions. Animal care and experimental procedures followed the guidelines of the Institutional Animal Care and Use Committee of the New York University School of Medicine and the Marine Biological Laboratory.

In Vivo EEG/LFP Recordings. Differential EEG or EEG/LFP recordings were performed in 11- to 13-wk-old mice. Details of survival surgery, EEG/LFP conditions, and data acquisition are given in *SI Materials and Methods*.

Data Analysis. Mean spectral power was calculated in 0.5-Hz bins (fast Fourier transform with Hamming window) using Clampfit software version 10.2 (Molecular Devices) from artifact-free 5-min EEG or LFP recordings made from each animal. Coherence and bispectral analysis were done using MATLAB (MathWorks, Inc.), and the squared normalized version was used for the visualizations. For details, see *SI Materials and Methods*.

Loss of Righting Reflex. Either ketamine (120 mg/kg) or ethanol (3.5 g/kg) was injected intraperitoneally, and individual mice were placed immediately in a Plexiglas cage. For details, see *SI Materials and Methods*.

Statistical analysis. Differences were considered significant if at least $P < 0.05$. Statistics were conducted with SigmaPlot-SigmaStat (version 12.0). All data values in text and figures are presented as means ± SEM. For details, see *SI Materials and Methods*.

ACKNOWLEDGMENTS. We thank Kerry D. Walton for helpful suggestions regarding the manuscript; Kenji Sakimura for providing $Ca_V3.1$ heterozygous mice; Daniel Johnson (Marine Biological Laboratory) for mice care; Eunjin Hwang for advising on coherence analysis; Hyungju Hwang for analysis of cross-bispectral coherence; and Mary Clarke for research administration. This work was supported by National Institutes of Health Grant NS13742/ NS/NINDS/NIH HHS (to R.R.L.) and a Postdoctoral Program Research Grant from University of Science and Technology in Republic of Korea (to S.C.).

1. Llinás R, Ribary U (2001) Consciousness and the brain. The thalamocortical dialogue in health and disease. *Ann N Y Acad Sci* 929:166–175.
2. Roy S, Llinás R (2008) Dynamic geometry, brain function modeling, and consciousness. *Prog Brain Res* 168:133–144.
3. Laureys S, et al. (1999) Impaired effective cortical connectivity in vegetative state: Preliminary investigation using PET. *Neuroimage* 9(4):377–382.
4. Sheeba JH, Stefanovska A, McClintock PV (2008) Neuronal synchrony during anesthesia: A thalamocortical model. *Biophys J* 95(6):2722–2727.
5. Arthuis M, et al. (2009) Impaired consciousness during temporal lobe seizures is related to increased long-distance cortical-subcortical synchronization. *Brain* 132(Pt 8): 2091–2101.
6. Carbone E, Lux HD (1984) A low voltage-activated, fully inactivating Ca channel in vertebrate sensory neurones. *Nature* 310(5977):501–502.
7. Llinás R, Yarom Y (1981) Electrophysiology of mammalian inferior olivary neurones in vitro. Different types of voltage-dependent ionic conductances. *J Physiol* 315: 549–567.
8. Jahnsen H, Llinás R (1984) Ionic basis for the electro-responsiveness and oscillatory properties of guinea-pig thalamic neurones in vitro. *J Physiol* 349:227–247.
9. Jahnsen H, Llinás R (1984) Electrophysiological properties of guinea-pig thalamic neurones: An in vitro study. *J Physiol* 349:205–226.
10. Cheong E, Shin HS (2013) T-type Ca2+ channels in normal and abnormal brain functions. *Physiol Rev* 93(3):961–992.
11. Kim D, et al. (2001) Lack of the burst firing of thalamocortical relay neurons and resistance to absence seizures in mice lacking alpha(1G) T-type Ca(2+) channels. *Neuron* 31(1):35–45.
12. Song I, et al. (2004) Role of the alpha1G T-type calcium channel in spontaneous absence seizures in mutant mice. *J Neurosci* 24(22):5249–5257.
13. Lee J, Kim D, Shin HS (2004) Lack of delta waves and sleep disturbances during non-rapid eye movement sleep in mice lacking alpha1G-subunit of T-type calcium channels. *Proc Natl Acad Sci USA* 101(52):18195–18199.
14. Anderson MP, et al. (2005) Thalamic Cav3.1 T-type Ca2+ channel plays a crucial role in stabilizing sleep. *Proc Natl Acad Sci USA* 102(5):1743–1748.
15. Kim U, Bal T, McCormick DA (1995) Spindle waves are propagating synchronized oscillations in the ferret LGNd in vitro. *J Neurophysiol* 74(3):1301–1323.
16. Lee J, et al. (2013) Sleep spindles are generated in the absence of T-type calcium channel-mediated low-threshold burst firing of thalamocortical neurons. *Proc Natl Acad Sci USA* 110(50):20266–20271.
17. Talley EM, et al. (1999) Differential distribution of three members of a gene family encoding low voltage-activated (T-type) calcium channels. *J Neurosci* 19(6):1895–1911.
18. Oh SW, et al. (2014) A mesoscale connectome of the mouse brain. *Nature* 508(7495): 207–214.
19. Llinás R, Jahnsen H (1982) Electrophysiology of mammalian thalamic neurones in vitro. *Nature* 297(5865):406–408.
20. Zhang Y, Llinas RR, Lisman JE (2009) Inhibition of NMDARs in the nucleus reticularis of the thalamus produces delta frequency bursting. *Front Neural Circuits* 3:20.
21. Jia F, Chandra D, Homanics GE, Harrison NL (2008) Ethanol modulates synaptic and extrasynaptic GABAA receptors in the thalamus. *J Pharmacol Exp Ther* 326(2): 475–482.
22. Ball GJ, Gloor P, Schaul N (1977) The cortical electromicrophysiology of pathological delta waves in the electroencephalogram of cats. *Electroencephalogr Clin Neurophysiol* 43(3):346–361.
23. Llinás RR, Grace AA, Yarom Y (1991) In vitro neurons in mammalian cortical layer 4 exhibit intrinsic oscillatory activity in the 10- to 50-Hz frequency range. *Proc Natl Acad Sci USA* 88(3):897–901.
24. Buzsáki G, Wang XJ (2012) Mechanisms of gamma oscillations. *Annu Rev Neurosci* 35: 203–225.
25. McCormick DA, McGinley MJ, Salkoff DB (2015) Brain state dependent activity in the cortex and thalamus. *Curr Opin Neurobiol* 31:133–140.
26. Hobson JA, Pace-Schott EF (2002) The cognitive neuroscience of sleep: Neuronal systems, consciousness and learning. *Nat Rev Neurosci* 3(9):679–693.
27. Pedroarena C, Llinás R (1997) Dendritic calcium conductances generate high-frequency oscillation in thalamocortical neurons. *Proc Natl Acad Sci USA* 94(2):724–728.
28. Llinás RR, Choi S, Urbano FJ, Shin HS (2007) Gamma-band deficiency and abnormal thalamocortical activity in P/Q-type channel mutant mice. *Proc Natl Acad Sci USA* 104(45):17819–17824.
29. Bartos M, Vida I, Jonas P (2007) Synaptic mechanisms of synchronized gamma oscillations in inhibitory interneuron networks. *Nat Rev Neurosci* 8(1):45–56.
30. Belluscio MA, Mizuseki K, Schmidt R, Kempter R, Buzsáki G (2012) Cross-frequency phase-phase coupling between θ and γ oscillations in the hippocampus. *J Neurosci* 32(2):423–435.
31. Schroeder CE, Lakatos P (2009) Low-frequency neuronal oscillations as instruments of sensory selection. *Trends Neurosci* 32(1):9–18.
32. Petrenko AB, Tsujita M, Kohno T, Sakimura K, Baba H (2007) Mutation of alpha1G T-type calcium channels in mice does not change anesthetic requirements for loss of the righting reflex and minimum alveolar concentration but delays the onset of anesthetic induction. *Anesthesiology* 106(6):1177–1185.